

Sequentially Evaporated Thin Film $\text{YBa}_2\text{Cu}_3\text{O}_{7-x}$ Superconducting Microwave Ring Resonator

Norman J. Rohrer, Hing Y. To, and George J. Valco
Ohio State University
Columbus, Ohio

Kul B. Bhasin
Lewis Research Center
Cleveland, Ohio

Chris Chorey
Sverdrup Technology, Inc.
Lewis Research Center Group
Brook Park, Ohio

Joseph D. Warner
Lewis Research Center
Cleveland, Ohio

Prepared for the
Conference on the Science and Technology of Thin Film Superconductors
sponsored by the U.S. Department of Energy
Denver, Colorado, April 30—May 4, 1990

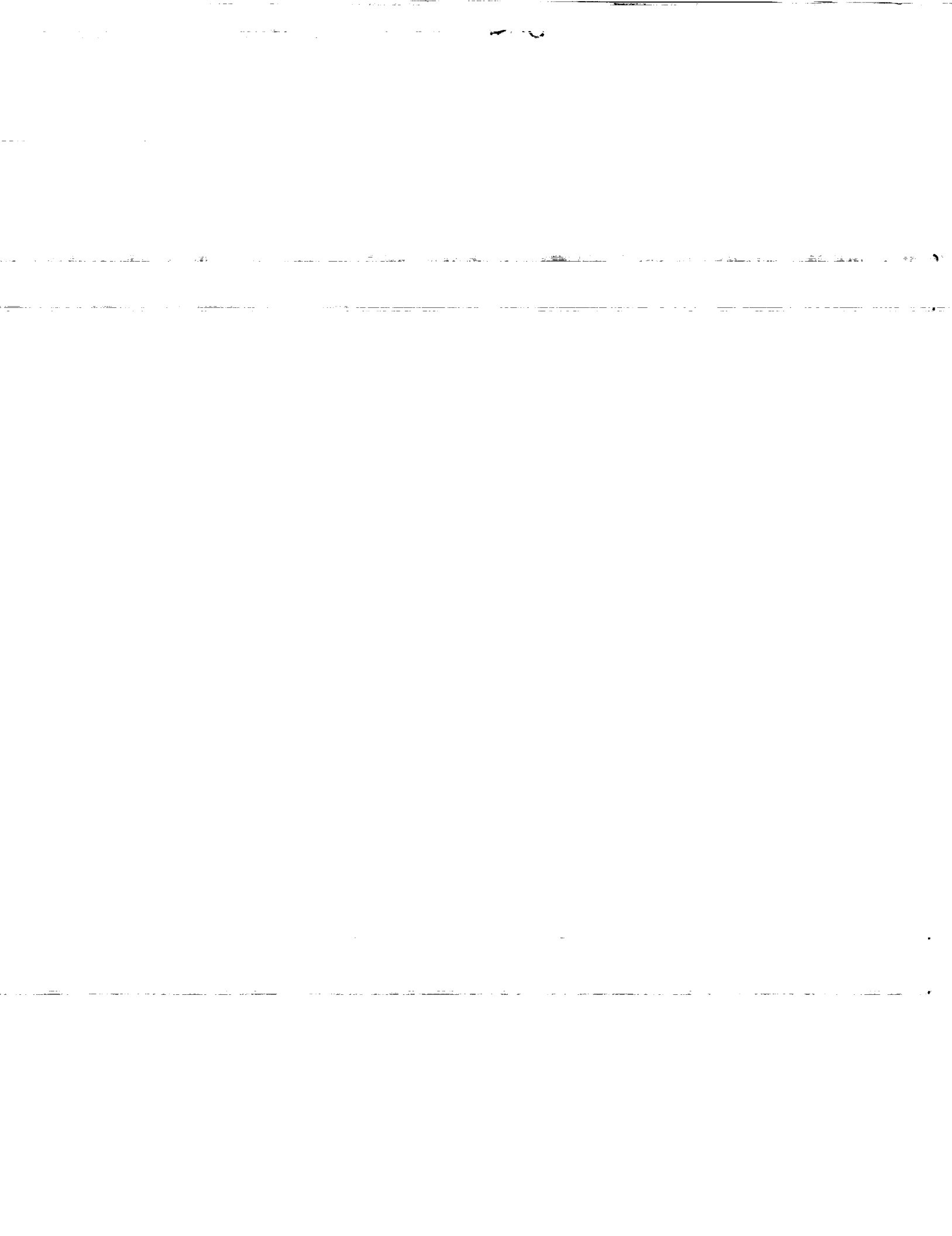


(NASA-TM-103180) SEQUENTIALLY EVAPORATED
THIN FILM $\text{YBa}_2\text{Cu}_3\text{O}_{7-x}$ SUPERCONDUCTING
MICROWAVE RING RESONATOR (NASA) 12 p

CSCL 09A

N90-25273

Unclas
G3/33 0289154



SEQUENTIALLY EVAPORATED THIN FILM $\text{YBa}_2\text{Cu}_3\text{O}_{7-x}$
SUPERCONDUCTING MICROWAVE RING RESONATOR

Norman J. Rohrer, Hing Y. To, and George J. Valco

Department of Electrical Engineering
Ohio State University, Columbus, Ohio 43210

Kul B. Bhasin

National Aeronautics and Space Administration
Lewis Research Center, Cleveland, Ohio 44135

Chris Chorey

Sverdrup Technology, Inc.
Lewis Research Center Group, Brook Park, Ohio 44142

Joseph D. Warner

National Aeronautics and Space Administration
Lewis Research Center, Cleveland, Ohio 44135

ABSTRACT

There is great interest in the application of thin film high temperature superconductors in high frequency electronic circuits. A ring resonator provides a good test vehicle for assessing the microwave losses in the superconductor and for comparing films made by different techniques. Ring resonators made of $\text{YBa}_2\text{Cu}_3\text{O}_{7-x}$ have been investigated on LaAlO_3 substrates. The superconducting thin films were deposited by sequential electron beam evaporation of Cu, Y, and BaF_2 with a post anneal. Patterning of the superconducting film was done using negative photolithography. A ring resonator was also fabricated from a thin gold film as a control. Both resonators had a gold ground plane on the backside of the substrate. The ring resonators' reflection coefficients were measured as a function of frequency from 33 to 37 GHz at temperatures ranging from 20 K to 68 K. The resonator exhibited two resonances which were at 34.5 and 35.7 GHz at 68 K. The resonant frequencies increased with decreasing temperature. The magnitude of the reflection coefficients is used in the calculation of the unloaded Q-values. The performance of the evaporated and gold resonator are compared with the performance of a laser ablated $\text{YBa}_2\text{Cu}_3\text{O}_{7-x}$ resonator. The causes of the double resonance are discussed.

INTRODUCTION

The advent of high temperature superconductors has drawn attention towards the possibilities of using thin films superconductors in microwave circuits. Several measurement techniques have been employed for characterization of the films including high Q cavities [1], stripline resonators [2] and

ring resonators [3]. The surface resistance of the the YBa₂Cu₃O_{7-x} superconductor has been investigated on bulk samples, thin films and single crystals [4-6]. In this paper we employ a ring resonator to study the microwave properties of YBa₂Cu₃O_{7-δ} fabricated by multi-layer sequential evaporation with post-anneal.

DEPOSITION AND ANNEAL PROCEDURES

Electron beam evaporation was used for deposition of Cu, Y, and BaF₂ on LaAlO₃. The materials were deposited in that order which was repeated four times for a total of twelve layers. The thicknesses of the individual layers were 507 angstroms for Cu, 473 angstroms for Y, and 1704 angstroms for BaF₂. The details of the deposition process have been previously reported [7,8].

The multilayer stack was subjected to a post anneal to assist in the formation of the proper phase of YBa₂Cu₃O_{7-x}. The samples were inserted into a preheated furnace using a slow push. They were annealed at 900 °C for 45 minutes in oxygen bubbled through room temperature water. The temperature was then ramped down to 450 °C where it was held for six hours. Finally, the temperature was ramped down to room temperature. The ambient was dry oxygen during all stages except the high temperature anneal. This procedure resulted in a one micron thick superconducting thin film with an onset temperature of 93 K and a critical temperature of 85 K.

PATTERNING PROCEDURE

The ring resonator was patterned using negative photolithography. KTI 752 photoresist was spun on at a rate of 4,000 rpm for 60 seconds which resulted the photoresist being 1.7 μm thick. The sample was soft baked at 95 °C for 25 minutes and exposed through a dark field mask for five seconds with an illumination power density of 34.8 mW/cm². The photoresist was developed for 2 minutes and 45 seconds in 802 developer and rinsed in ethanol. A one percent molar bromine solution in ethanol was used for etching the thin film followed by a 30 second rinse. Finally, the photoresist was removed in SN-10 stripper.

Once the superconductor was patterned, a ground plane was deposited on the back of the substrate using electron beam evaporation. For adhesion, a 1400 angstrom titanium layer was deposited before the one micron gold ground plane.

RESONATOR ANALYSIS

The following dimensions correspond to the resonator shown in Figure 1. H is the substrate thickness.

$$\begin{array}{ll} H = 254 \text{ microns} & W = 143.3 \text{ microns} \\ S = 36 \text{ microns} & R = (r_1 + r_2)/2 = 990 \text{ microns} \end{array}$$

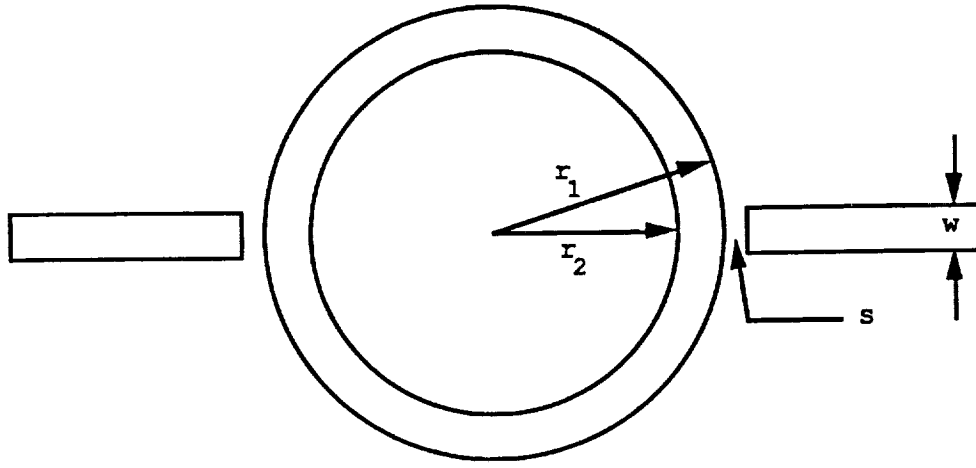


Figure 1: Ring resonator.

The resonator was designed for 50 ohm transmission lines with a resonant frequency of 30 GHz for the first harmonic. At the time of the design, the dielectric constant for LaAlO_3 was reported to be 15. Since then a more recent value reported for the dielectric constant is 21.9. This has resulted in a characteristic impedance for this geometry 42.9 ohms. The first harmonic was decreased below K-band. For this reason, we measured at the second harmonic which had a resonant frequency of 35.1 GHz at 25 K.

Microwave Testing

Once fabricated the ring resonator was experimentally tested using an HP 8510B network analyzer. The microwave test setup was configured using waveguides. Thus, a waveguide to microstrip transition was implemented using a cosine tapered ridge transition [9].

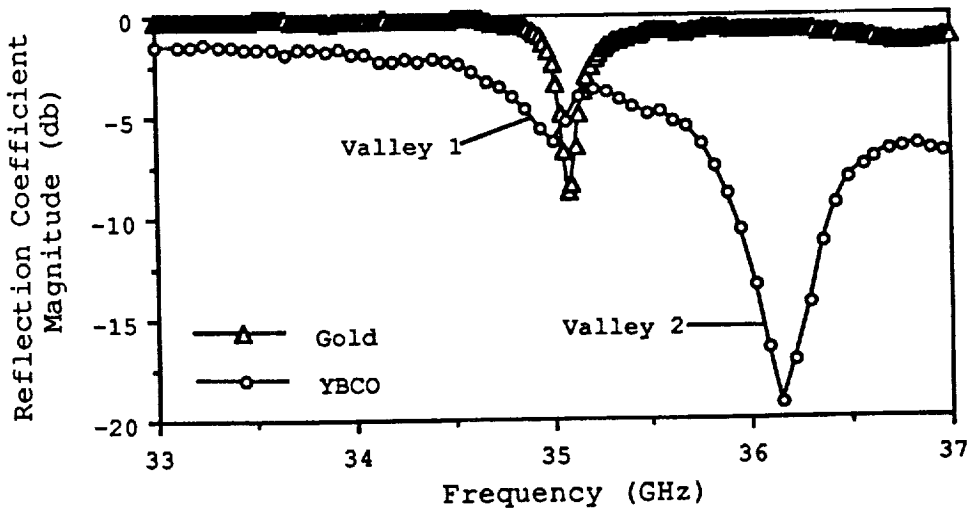


Figure 2: Magnitude of the reflection coefficient for ring resonator's fabricated from gold and $\text{YBa}_2\text{Cu}_3\text{O}_{7-x}$ at 30 K.

The reflection coefficient for the resonators was measured as a function of frequency at temperatures ranging from 20 K to 300 K using a CTI closed cycle cryogenic refrigerator. The superconducting resonator was measured from 20 K to its critical temperature. The resonant frequency superconducting resonator was 35.1 GHz at 25 K. Figure 2 shows the magnitude of the reflection coefficient for both the gold and the superconducting resonator at approximately 30 K.

The superconducting resonator exhibited two resonant valleys. Valley 1 matched the resonant frequency of the gold resonator while valley 2 occurred at 36.1 GHz. As will be discussed below, the occurrence of the second valley can be caused by one section of the ring resonator having a larger impedance than the rest of the ring.

Double Resonance Modeling

A transmission line model was implemented in Touchstone [10] to allow study of the double resonance. The resonator was simulated using transmission lines to match the physical layout and capacitors to model the gap. The capacitance values used were calculated from empirical equations derived in reference [11]. The impedance was increased in a region corresponding to three percent of the ring's circumference located closer to the transmission end. The location of this section for our model was 114° from the input. The impedance of this region was increased from a single line with 42.9 ohms to two parallel lines of 150 ohms each. This simulates a blister centered in the ring's transmission line. Figure 3 presents the results from this model.

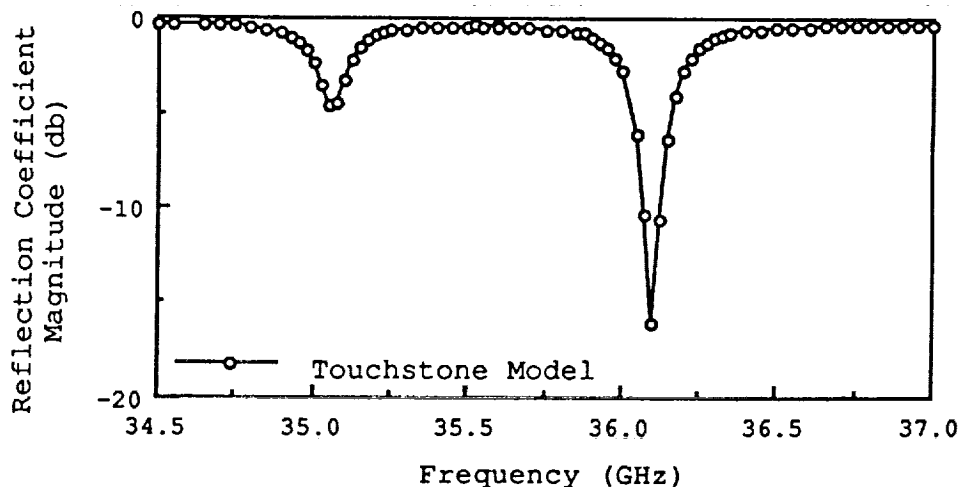


Figure 3: Modeled ring resonator with blister centered in the transmission line. Impedance of the lines around the blister were 150 ohms. Blister was located 1/3 the way around the ring.

The resonant frequencies of the model match directly with the resonant frequencies of the superconducting ring resonator. The width of valley 1 is quite similar, but the width of valley 2 is smaller for the modeled resonator. The reflection coefficient is much lower off resonance for the superconducting resonator. The the depth of the valley's peaks could be

altered by varying the position of the blister around the ring. The position used for the calculation shown in Figure 3 agrees with the location of a blistered region observed in the film of the resonator. The separation of the two valleys could be increased by increasing the impedance of the transmission lines around the blister. The response of the model remained the same for different number of transmission lines used within the high impedance region as long as the parallel combination of the characteristic impedances remained constant.

Resonant Frequency Shifts

The group velocity for a microstrip configuration with superconducting transmission lines varies as a function of temperature for temperatures less than the superconductor's critical temperature. This corresponds directly to a change in wavelength. Thus, the resonant frequency also varies as a function of temperature. The group velocity for a superconducting transmission line with a superconducting ground plane is given by [12]

$$v = \frac{c}{\sqrt{e_{\text{eff}}(f)}} \left[1 + \left(\lambda_1/h \right) \coth \left(t_1/\lambda_1 \right) + \left(\lambda_2/h \right) \coth \left(t_2/\lambda_2 \right) \right]^{-1/2}$$

where λ_1 and t_1 are the transmission line's penetration depth and thickness, respectively, and λ_2 and t_2 are the ground plane's penetration depth and thickness, respectively. If the ground plane is a normal metal, the group velocity is reduced to

$$v = \frac{c}{\sqrt{e_{\text{eff}}(f)}} \left[1 + \left(\lambda_1/h \right) \coth \left(t_1/\lambda_1 \right) \right]^{-1/2}$$

Note that the first equation is general enough to accommodate microstrip circuitry with superconductors of different penetration depths for the transmission line and ground plane.

Figure 4 shows the calculated resonant frequency for a 0.7 micron thick film as a function of the temperature normalized to the critical temperature. This graph shows three plots. Two plots show the comparison of the resonant frequency with two different penetration depths for a sample with a gold ground plane and a superconducting resonator. The penetration depths were chosen to be on each side of the values experimentally determined by [13]. The third plot represented by the open squares shows the resonant frequency as a function of temperature for a sample with both the ground plane and the resonator being superconducting. Replacing both the transmission lines and the ground plane with a superconductor will decrease the losses in the circuit if the superconductor losses are lower than the gold losses. The resonant frequency for a sample with both a superconducting transmission line and a ground plane will exhibit a larger shift in the resonant frequency as the temperature nears the critical temperature for the superconducting film.

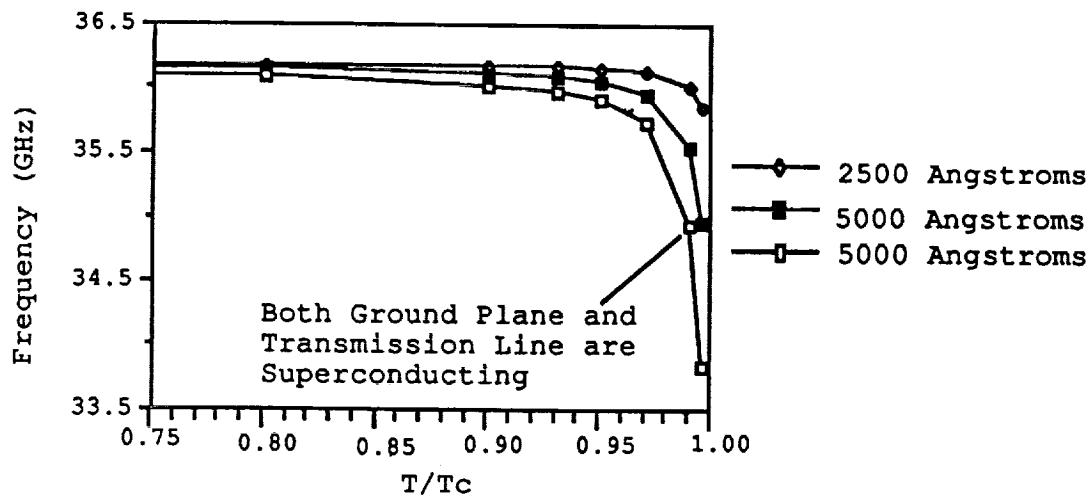


Figure 4: Resonant frequency versus normalized temperature for a 0.7 micron thick film. Different penetration depths are shown as well as an example of both ground plane and transmission lines being superconductors.

The shift in the resonant frequency for the sequentially evaporated superconducting ring resonator exhibited the same shape as the theoretical predictions. The measured resonant frequency as a function of temperature is given in Figure 5.

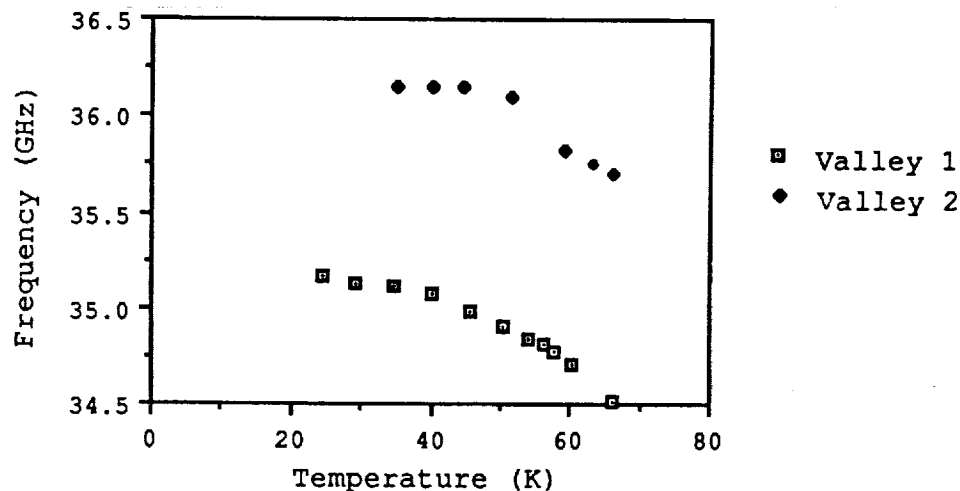


Figure 5: Resonant frequency versus temperature for the superconducting ring resonator. Both valleys are represented.

An attempt was performed to try to match the theoretical equations with the experimental data. The equations resulted in a penetration depth that was much larger than the thickness of the film. This is not reasonable since the film would no longer be superconducting for a large penetration depth. A possible explanation for the large penetration depth is due to the film being granular. This may allow more penetration at between grains.

Unloaded Q Calculation

The unloaded Q of the resonator can be extracted from the reflection coefficient. The model used for the derivation of the equation is a parallel RLC circuit with an ideal transformer in parallel and a series input resistance [14]. This model is for an unterminated resonator. It was used since the resonator was not loaded on the transmission side during our testing.

The derivation of the equations presented here are published in reference [14]. The loaded Q of a resonator is given by

$$Q_L = \frac{f_r}{f_1 - f_2}$$

where f_1 and f_2 are the half power points on each side of the resonant frequency f_r . The values for the half power levels are calculated by

$$P_{1/2} = \frac{1}{2} \left(\left[\frac{k' - 1}{k' + 1} \right]^2 + \left[\frac{\sigma - 1}{\sigma + 1} \right]^2 \right)$$

where σ is the coupling loss and k' is the effective coupling coefficient. The coupling loss is calculated far off resonance where the reflection coefficient (Γ_i) is nearly constant.

$$\sigma = \frac{1 - \Gamma_i}{1 + \Gamma_i}$$

The effective coupling coefficient is the sum of the coupling coefficient and the coupling loss. The coupling coefficient can be easily calculated using the reflection coefficient (Γ_r) at the resonant frequency. The coupling coefficient can be calculated by

$$k = \frac{1 - \Gamma_r}{1 + \Gamma_r} \quad \text{or} \quad k = \frac{1 + \Gamma_r}{1 - \Gamma_r}$$

for the undercoupled and overcoupled cases, respectively. The unloaded Q can be calculated from the loaded Q by

$$Q_o = Q_L \left(\frac{1 + k'}{1 + \sigma} \right)$$

The unloaded Q as a function of temperature is shown in Figure 6. The unloaded Q for both valleys of the sequentially evaporated resonator are shown.

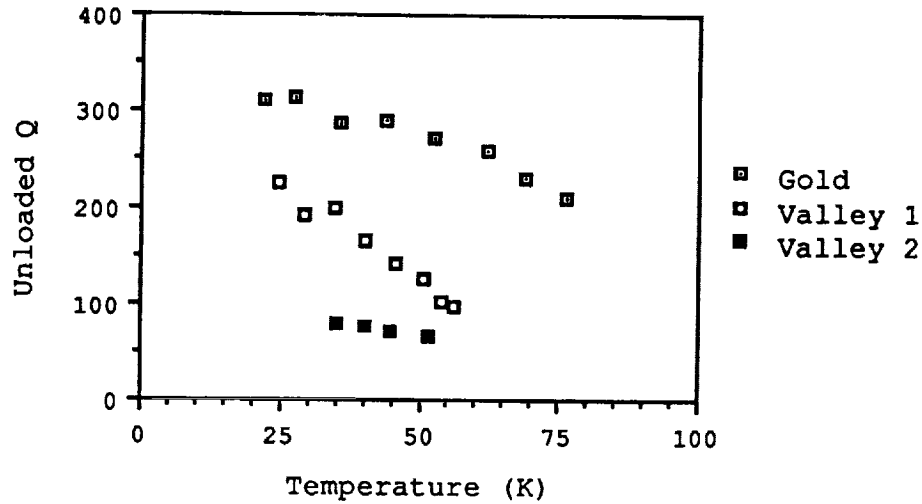


Figure 6: Unloaded Q versus temperature for the gold ring and the superconducting ring. Both valleys are shown for the superconducting ring.

The gold resonator had a larger unloaded Q than our sequentially evaporated film. At lower temperatures the difference between the unloaded Q values narrowed since the superconducting resonator's unloaded Q increased faster than the gold resonator's when compared to valley 1.

Surface Resistance

The surface resistance of the ring resonator can be extracted from the unloaded Q. The surface resistance is given by [15]

$$R_{ss} = R_{SAU} - \frac{4\pi Z_0}{B(C + D)} \frac{\pi}{\lambda} \left(\frac{1}{Q_{oAU}} - \frac{1}{Q_{oS}} \right)$$

where R_{SAU} is the surface resistance of gold, and Q_{oAU} and Q_{oS} are the unloaded Q values of the gold resonator and the superconducting resonator at the same temperature, respectively. The constants B, C, and D are related to the physical dimensions and are given in reference [15].

The surface resistance as a function of temperature for both the gold and the sequentially evaporated films are shown in Figure 7. For comparison a ring resonator was fabricated from a film deposited by laser ablation [16]. The surface resistance calculated for this film is also shown in Figure 7.

The graph shows that the sequentially evaporated film had the highest surface resistance at all temperatures. The gold film's surface resistance was about two-thirds the value of the sequentially evaporated film at 25 K. The laser ablated film had a surface resistance of approximately half that of gold at temperatures less than 50 K. As the temperature neared the critical temperature, the surface resistance of the laser ablated film started to increase rapidly to a value larger than that for gold at 70 K.

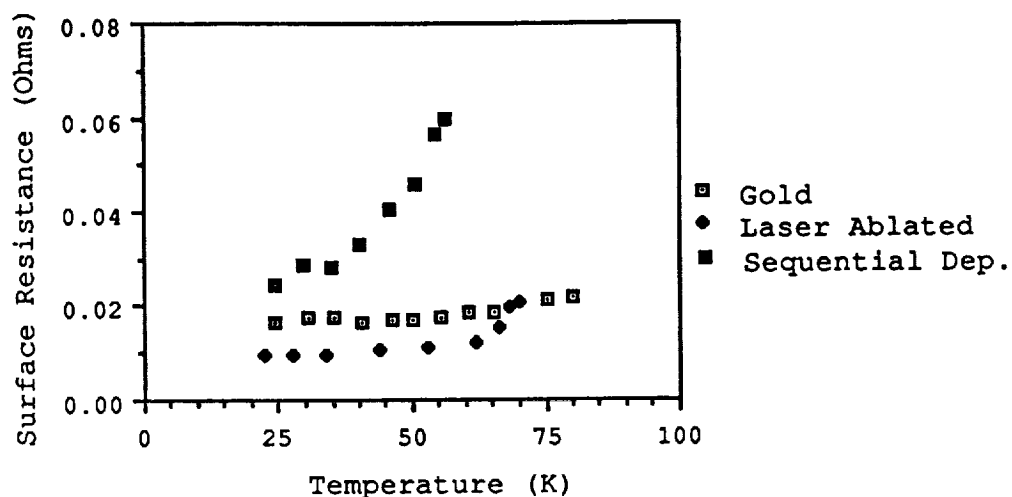


Figure 7: Surface resistance versus temperature for a gold resonator and two superconducting resonators. The superconducting resonators were deposited using different techniques. One was deposited by laser ablation and one by sequential evaporation.

CONCLUSION

A sequentially evaporated $\text{YBa}_2\text{Cu}_3\text{O}_{7-x}$ superconducting thin film was patterned into a ring resonator using negative photolithography. The ring resonators' reflection coefficients were measured using an HP 8510B network analyzer as a function of frequency from 33 to 37 GHz at temperatures ranging from 20 K to 68 K. The resonator exhibited two resonances which were at 34.5 and 35.7 GHz at 68 K. The resonant frequencies increased with decreasing temperature. The double resonance could be explained using a model that allowed for a small section of the ring resonator to have a larger impedance than the rest of the ring resonator. The location of the high impedance section in the model correlated well with the location of a blistered region of the film in the resonator. Once the reflection coefficient data was taken, the unloaded Q was extracted. The superconducting resonator was compared to a gold resonator. The gold resonator had a higher unloaded Q value at all temperatures. This translated into the gold having a lower surface resistance than the sequentially evaporated superconducting film. The surface resistance of the gold was about two-thirds the surface resistance of the sequentially evaporated superconducting film at 25 K. When compared to the laser ablated film, the laser ablated film's surface resistance was about one half that of gold for temperatures less than 50 K.

ACKNOWLEDGEMENTS

Design of the ring resonator was done by Robert Romanofsky and one of the authors (Kul Bhasin). This research was funded by the National Aeronautics and Space Administration, Lewis

REFERENCES

1. J. S. Marten, J. B. Beyer, and D. S. Ginley, Appl. Phys. Lett. **52** (21), 1822 (1988).
2. M. DiIorio, A. C. Anderson, and B. Y. Tsaur, Phys. Rev. B., **38** (10), 9726 (1988).
3. J. H. Takemoto, F. K. Oshita, H. R. Fetterman, P. Korbin, E. Sovero, **MTT-37**, 1650 (1989).
4. M. K. Wu, J. R. Ashburn, C. J. Torng, P. H. Hor, R. L. Meng, L. Gao, Z. J. Huang, Y. O. Wang, and C. W. Chue, Phys. Rev. Lett., **58**, 908 (1987).
5. T. M. P. Percival, J. S. Thorn, and R. Driver, Electron. Lett., **23**, 1225 (1987).
6. I. Sankawa, M. Sato, T. Konaka, M. Dobayashi, and K. Ishihara, Jap. Journ. Appl. Phys., **27** (9), L1637 (1988).
7. G. J. Valco, N. J. Rohrer, J. D. Warner and K. B. Bhasin, High T_c Superconducting Thin Films, Devices and Applications, G. Margaritondo, R. Joynt and M. Onellion, AIP Conference Proceedings No. 182, pp. 147-154, American Institute of Physics, Atlanta, 1988.
8. G. J. Valco, N. J. Rohrer, J. D. Warner and K. B. Bhasin, Proceedings of the Workshop on High Temperature Superconductivity, pp. 197-203, GACIAC, Hunstville, 1989.
9. R. R. Romanofsky and K. A. Shalkhauser, NASA Technical Paper # 2875, 1989.
10. Commercially available software, EEsof, Westlake Village, CA 91632.
11. R. Garg and J. J. Bahl, Int. Journ. Elect., **45** (1978).
12. J. C. Swihart, Journ. Appl. Phys., **32** (3), 461 (1961).
13. S. M. Anlage, H. Sze, H. J. Snortland, S. Tahara, B. Langley, C. B. Eom, M. R. Beasley, R. Taber, Appl. Phys. Lett. **54** (26) 1989.
14. Robert R. Romanofsky, NASA Technical Paper #2899, 1989.
15. J. Takamoto, F. Oshita, H. Fetterman, IEEE Trans., **MTT-37**, 1650 (1989).
16. K. B. Bhasin, C. M. Chorey, J. D. Warner, R. R. Romanofsky, V. O. Heinen, K. S. Kong, H. Y. Lee, and T. Itoh, To be published in Symp. Digest of the 1990 IEEE Int. Microwave Symp., Dallas, TX.

1. Report No. NASA TM-103180		2. Government Accession No.		3. Recipient's Catalog No.	
4. Title and Subtitle Sequentially Evaporated Thin Film $\text{YBa}_2\text{Cu}_3\text{O}_{7-x}$ Superconducting Microwave Ring Resonator				5. Report Date	
				6. Performing Organization Code	
7. Author(s) Norman J. Rohrer, Hing Y. To, George J. Valco, Kul B. Bhasin, Chris Chorey, and Joseph D. Warner				8. Performing Organization Report No. E-5557	
				10. Work Unit No. UPI307-51-00	
9. Performing Organization Name and Address National Aeronautics and Space Administration Lewis Research Center Cleveland, Ohio 44135-3191				11. Contract or Grant No.	
				13. Type of Report and Period Covered Technical Memorandum	
12. Sponsoring Agency Name and Address National Aeronautics and Space Administration Washington, D.C. 20546-0001				14. Sponsoring Agency Code	
15. Supplementary Notes Prepared for the Conference on the Science and Technology of Thin Film Superconductors sponsored by the U.S. Department of Energy, Denver, Colorado, April 30—May 4, 1990. Norman J. Rohrer, Hing Y. To, George J. Valco, Department of Electrical Engineering, Ohio State University, Columbus, Ohio 43210. Kul B. Bhasin and Joseph D. Warner, NASA Lewis Research Center. Chris Chorey, Sverdrup Technology, Inc., Lewis Research Center Group, 2001 Aerospace Parkway, Brook Park, Ohio 44142.					
16. Abstract There is great interest in the application of thin film high temperature superconductors in high frequency electronic circuits. A ring resonator provides a good test vehicle for assessing the microwave losses in the superconductor and for comparing films made by different techniques. Ring resonators made of $\text{YBa}_2\text{Cu}_3\text{O}_{7-x}$ have been investigated on LaAlO_3 substrates. The superconducting thin films were deposited by sequential electron beam evaporation of Cu, Y, and BaF_2 with a post anneal. Patterning of the superconducting film was done using negative photolithography. A ring resonator was also fabricated from a thin gold film as a control. Both resonators had a gold ground plane on the backside of the substrate. The ring resonators' reflection coefficients were measured as a function of frequency from 33 to 37 GHz at temperatures ranging from 20 K to 68 K. The resonator exhibited two resonances which were at 34.5 and 35.7 GHz at 68 K. The resonant frequencies increased with decreasing temperature. The magnitude of the reflection coefficients is used in the calculation of the unloaded Q-values. The performance of the evaporated and gold resonator are compared with the performance of a laser ablated $\text{YBa}_2\text{Cu}_3\text{O}_{7-x}$ resonator. The causes of the double resonance are discussed.					
17. Key Words (Suggested by Author(s)) Superconducting thin films Sequential evaporation Microwave passive circuits			18. Distribution Statement Unclassified—Unlimited Subject Category 33		
19. Security Classif. (of this report) Unclassified		20. Security Classif. (of this page) Unclassified		21. No. of pages 12	
				22. Price* A03	

